[redacted]

[redacted] RECEIVED

AUG - 4 1995

FEDERAL COMMUNICATIONS COMMISSION
OFFICE OF SECRETARY

Before the
FEDERAL COMMUNICATIONS COMMISSION
Washington, D.C. 20554

In the Matter of	)	
	)	
Preparation for International	)	IC Docket No. 94-31
Telecommunication Union World	)	
Radiocommunication Conferences	)	

DOCKET FILE COPY ORIGINAL

[redacted] FURTHER SUPPLEMENTAL COMMENTS
OF LEO ONE USA CORPORATION

Leo One USA Corporation ("Leo One USA"), by counsel, hereby submits these Further Supplemental Comments in the above-captioned proceeding. Leo One USA is a pending applicant for a mobile satellite service ("MSS") below 1 GHz system. It has actively participated in this proceeding including the submission of Comments and Reply Comments. In its Reply Comments, Leo One USA indicated that it was undertaking detailed sharing studies for MSS below 1 GHz systems and that the results of those studies would be forwarded to the Commission when complete. On July 6, 1995, Leo One USA submitted a Report on uplink sharing. The Downlink Report is now finished and is being submitted herewith.

This study analyzes the feasibility of operating non-voice non-geostationary ("NVNG") mobile satellite service ("MSS") downlinks in various VHF and UHF bands. The results of this study show that NVNG MSS systems can successfully operate their downlinks in several VHF and UHF bands.

For this study, field measurements were taken to characterize the statistics of the total noise power present in the Leo One USA communications downlink band relative to the

No. of Copies rec'd 0+5
List ABCDE

thermal noise background. Human-made and environmental noise power measurements were made at various fixed sites and from a moving vehicle in the Los Angeles area.[1] Measurements were taken for various representative environments as a function of time-of-day and band center frequency. The measurement data was processed numerically to obtain the exceedence probability distribution of the measured total noise power to thermal noise power ratio, $Y = 10\log^{10}(N/n)$. Here N denotes the total measured noise power and $n = kT^{\circ}B$ is the background noise power as seen in a bandwidth $B = 25$ kHz, where k is Boltzmann's constant and T° is the equivalent thermal noise temperature in degrees Kelvin.

The measured exceedence probability distribution, $P(Y \leq y)$, was then used to calculate the percent of time that the total noise power to thermal noise power ratio exceeds various values of interest. The percentages evaluated were the 10%, the 50% (median), and the 90% points, the corresponding values of the total noise power to thermal noise power ratio, are $Y_{0.1}$, $Y_{0.5}$ and $Y_{0.9}$. Additionally, the intervals $[Y_{0.9}, Y_{0.1}]$ in which the total noise power ratios remain 80% of the time were obtained. From the measurements of Y, one can readily conclude that the total noise power to thermal noise power ratios experienced will not

---

[1] The noise measurement equipment was installed in a truck and a 6" VHF/UHF antenna was mounted vertically at the back of the passenger section of the truck. The truck and the antenna were selected to represent a typical Leo One USA mobile installation.

pose serious operational problems with respect to Leo One USA downlink communications. Thus, NVNG MSS systems can successfully operate in the bands between 100-500 MHz.

Respectfully submitted,

Robert A. Mazer
ROSENMAN & COLIN
1300 19th Street, N.W., Suite 200
Washington, D.C. 20036
(202) 463-4645

Dated: August 4, 1995

Attorney for Leo One USA Corporation

CERTIFICATE OF SERVICE

I, Robert A. Mazer, do hereby certify that a true and correct copy of the foregoing "Further Supplemental Comments of Leo One USA Corporation" was sent by first-class mail, postage prepaid, or hand-delivered*, on this 4th day of August, 1995, to the following persons.

Chairman Reed E. Hundt*
Federal Communications Commission
1919 M Street, N.W., Room 814
Washington, DC 20554

Commissioner James H. Quello*
Federal Communications Commission
1919 M Street, N.W., Room 802
Washington, DC 20554

Commissioner Andrew C. Barrett*
Federal Communications Commission
1919 M Street, N.W., Room 826
Washington, DC 20554

Commissioner Rachelle B. Chong*
Federal Communications Commission
1919 M Street, N.W., Room 844
Washington, DC 20554

Commissioner Susan Ness*
Federal Communications Commission
1919 M Street, N.W., Room 832
Washington, DC 20554

Mr. Scott Blake Harris, Chief*
International Bureau
Federal Communications Commission
2000 M Street, N.W., Room 830
Washington, DC 20554

Thomas S. Tycz, Division Chief*
Satellite & Radiocommunication Division
International Bureau
Federal Communications Commission
2000 M Street, N.W., Room 811
Washington, DC 20554

Mr. Steven Selwyn*
Federal Communications Commission
2000 M Street, N.W., Room 811
Washington, DC 20554

Mr. Ronald Netro*
Wireless Telecommunications Bureau
Federal Communications Commission
2025 M Street, N.W., Room 5002
Washington, DC 20554

Mr. Richard D. Parlow*
Office of Spectrum
National Telecommunications &
Information Administration
Department of Commerce
14th St. & Constitution Ave., N.W.,
Room 4099
Washington, DC 20230

Mr. William D. Gamble*
Deputy Associate Administrator
National Telecommunications &
Information Administration
Department of Commerce
14th St. & Constitution Ave., N.W.,
Room 4099
Washington, DC 20230

Mr. Warren Richards*
U.S. Department of State
2201 C Street, N.W.
Washington, DC 20520

Ms. Carolyn Darr*
Associate Administrator
Office of International Affairs/NTIA
U.S. Department of Commerce
14th & Constitution Ave., N.W., Room 4720
Washington, DC 20230

Cecily C. Holiday, Deputy Division Chief*
Satellite & Radiocommunication Division
International Bureau
Federal Communications Commission
2000 M Street, N.W., Room 520
Washington, DC 20554

Fern J. Jarmulnek, Branch Chief*
Satellite Policy Branch
Satellite & Radiocommunication Division
International Bureau
Federal Communications Commission
2000 M Street, N.W., Room 518
Washington, DC 20554

Kristi Kendall, Esquire*
Satellite Policy Branch
Satellite & Radiocommunication Division
International Bureau
Federal Communications Commission
2000 M Street, N.W., Room 517
Washington, DC 20554

Harold Ng, Branch Chief*
International Bureau
Federal Communications Commission
2000 M Street, N.W., Room 512
Washington, DC 20554

Mr. William Luther, Branch Chief*
Radiocommunication Policy Branch
International Bureau
Federal Communications Commission
2000 M Street, N.W., Room 804
Washington, DC 20554

Mr. Damon C. Ladson*
International Bureau
Federal Communications Commission
2000 M Street, N.W., Room 803
Washington, DC 20554

Mr. Al Schneider*
Federal Communications Commission
1919 M Street, N.W., Room 408
Washington, DC 20554

Thomas J. Keller, Esquire
Verner Liipfert Bernhard
McPherson & Hand, Chartered
901 15th Street, N.W., Suite 700
Washington, DC 20005

Carl R. Frank, Esquire
Wiley, Rein & Fielding
1776 K Street, N.W.
Washington, DC 20006

William K. Keane, Esquire
Winston & Strawn
1400 L Street, N.W.
Washington, DC 20005

L. R. Raish, Esquire
Fletcher, Heald & Hildreth
1300 N. 17th Street, 11th Floor
Rosslyn, VA 22209

Mr. Robert L. Hoggarth, Director
Regulatory Relations
PCIA
1501 Duke Street
Alexandria, VA 22314-3450

Mr. Jeffrey Sheldon
UTC
1140 Connecticut Avenue, N.W., Suite 1140
Washington, DC 20036

Mr. Richard Barth, Director
Office of Radio Frequency Management
National Oceanic and Atmospheric Administration
Federal Building 4
Suitland, MD 20233

Julie T. Barton, Esquire
Hogan & Hartson, L.L.P.
555 13th Street, N.W.
Washington, DC 20004-1109

Robert L. Riemer
Senior Program officer
National Research Council
2101 Constitution Avenue, N.W.
Washington, DC 20418

Dennis J. Burnett, Esquire
Hight, Gardner, Poor & Havens
1301 I Street, N .W., Suite 470E
Washington, DC 20005

Leslie A. Taylor, Esquire
Leslie Taylor Associates
6800 Carlynn Court
Bethesda, MD 20817-4301

Jill Abeshouse Stern, Esquire
Shaw, Pittman, Potts & Trowbridge
2300 N Street, N.W.
Washington, DC 20037

Albert Halprin, Esquire
Halprin, Temple & Goodman
Suite 650 East Tower
1100 New York Avenue, N.W.
Washington, DC 20005

Mr. Mark J. Golden
Personal Communications Industry Association
1019 19th Street, N.W., Suite 1100
Washington, DC 20036

Robert M. Gurss, Esquire
Wilkes, Artis, Hedrick & Lane, Chtd.
1666 K Street, N.W., Suite 1100
Washington, DC 20006

Raul R. Rodriguez, Esq.
Leventhal, Senter & Lerman
2000 K Street, N.W., Suite 600
Washington, DC 20006

Ronald J. Jarvis, Esquire
Catalano & Jarvis, P.C.
1101 30th Street, N.W., Suite 300
Washington, DC 20007

Robert A. Mazer

Robert A. Mazer

Leo One USA

Downlink Band

Noise Measurements

Prepared by:

Mark A. Sturza
Leo One USA

Steve Kuh
Allan Uy
LinCom Corporation

24 July 1995

LinCom
CORPORATION

5110 W. Goldleaf Circle, Suite 330 Los Angeles, CA 90056 Phone 213-293-3001 Fax 213-293-3063
TM-LEO-95025

Table of Contents

1.0 Introduction and Summary

This study analyzes the feasibility of operating non-voice non-geostationary (NVNG) mobile satellite service (MSS) downlinks in various VHF and UHF bands. Noise measurements were made at various locations in the Los Angeles area. The results of this study show that NVNG MSS systems can successfully operate their downlinks in several VHF and UHF bands not shared with terrestrial services.

Leo One USA proposes to operate its subscriber downlinks in the 137 - 138 MHz frequency band. Other bands from 100 MHz to 500 MHz are also being considered for NVNG MSS downlinks. Unlike the uplink bands, where sharing with terrestrial services is possible, NVNG MSS systems generally cannot share their subscriber downlink spectrum with terrestrial services. Nearby terrestrial transmitters would jam the weak signals from far-off satellites. Thus noise from intentional transmissions is not an issue.

In these bands, human-made noise typically sets the noise level for subscriber transceiver reception of the downlink signal. The dominant noise source is automotive noise, followed by noise from power-generating facilities, and then noise from industrial equipment. Other noise sources, such as consumer products, lighting systems, medical equipment, electric trains, and buses are generally too low to be of concern.

Human-made and environmental noise power measurements were made at various fixed sites and from a moving vehicle in the Los Angeles area. The noise measurement equipment was installed in a truck and a 6" VHF/UHF antenna was mounted vertically at the back of the passenger section of the truck. The truck and the antenna were selected to represent a typical Leo One USA mobile installation.

The measurement setup and measurement locations are described in Sections 2 and 3, respectively. For the fixed site measurements, the vehicle was parked at locations representative of 8 different environment, see Table 1-1. Summaries of these measurements can be found in Section 4. Six to nine sets of measurements were generated each day with a spacing of fifteen minutes between each set. For the mobile cases, selected routes on the Los Angeles Freeway system were chosen. Summaries of these mobile measurements can be found in Section 5.

Table 1-1 shows the worst case noise measurements for each of the environments at the 90-th percentile level, only 10% of the measurements were above this value. The table lists the total measured noise power in a 25 KHz bandwidth in dB relative to just the thermal noise power contained in that 25 kHz bandwidth. The thermal noise power was calibrated each day. For example, in the case of the industrial environment, the worst case noise measurement indicates that there is a 10% chance that the human-made noise power will exceed the thermal noise power by 9.5 dB. For all measurements, the average (thermal) noise power measurement was -126 dBm in a 25 kHz bandwidth.

Environment	Frequency (MHz)	Human Made Noise Power Above kTB 10% of Time
Airport	137.4725	12.5
Industrial	137.4725	9.5
Urban	137.4445	10.5
Rural	388.1	9.3
Suburban	405.237	9.5
Harbor	137.0125	10.7
Freeway	137.4175	9
Reference	137.4175	8.7
Freeway Route 1	402.5	8.8
Freeway Route 2	388.1	9.9
Freeway Route 3	137.4175	24.6

Table 1-1. Worst Case Noise Measurement Summary

The noise power measurements can vary widely depending upon the time of day as shown in Figure 1-1. The noise power for each of the measurement frequencies are plotted over the course of a day while the measurement truck was driven on several freeways in the Los Angeles area. For example, the measurements corresponding to 137.0125 MHz show a variation of ~3dB. For the 388 MHz measurements, the noise measurement power increased during the heavy traffic hours. However, the largest noise power for 137.0125 MHz was measured during the early afternoon hours.

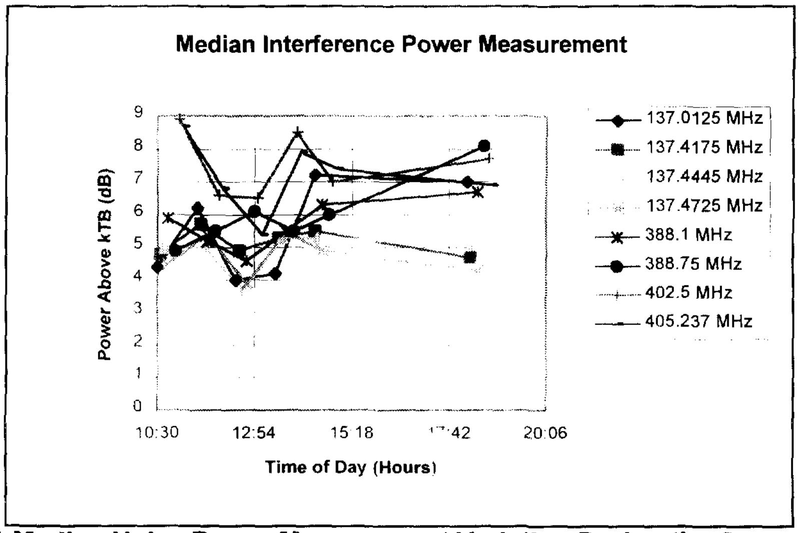

Figure 1-1 Median Noise Power Measurement Variation During the Course of a Day (Freeway Routes 4 and 5)

Tables showing all of the measurement data are provided in Appendix A. Appendix B contains plots of the measurement data. Measurements were also performed to characterize the parameters of the antenna being used. The results of these measurements are provided in Appendix C.

In conclusion, field measurements were taken to characterize the statistics of the total noise power present in the Leo One USA communications downlink band relative to the thermal noise background. Measurements were taken for various representative environments as a function of time-of-day and band center frequency. The measurement data was processed numerically to obtain the exceedence probability distribution of the measured total noise power to thermal noise power ratio, $Y = 10\log_{10}(N/\eta)$. Here N denotes the total measured noise power and $\eta = kT^{o}B$ is the background noise power as seen in a bandwidth B = 25 kHz, where k is Boltzmann's constant and T^{o} is the equivalent thermal noise temperature in degrees Kelvin.

The measured exceedence probability distribution, $P(Y \geq y)$, was then used to calculate the percent of time that the total noise power to thermal noise power ratio exceeds various values of interest. The percentages evaluated were the 10%, the 50% (median), and the 90% points, the corresponding values of the total noise power to thermal noise power ratio, are $y_{0.1}$, $y_{0.5}$, and $y_{0.9}$. Additionally, the intervals $[y_{0.9}, y_{0.1}]$ in which the total noise power to thermal noise power ratios remain 80% of the time were obtained. From the measurements of Y, one can readily conclude that the total noise power to thermal noise power ratios experienced will not pose serious operational problems with respect to Leo One USA downlink communications.

2.0 Measurement Setup and Theory

Figure 2-1 depicts the test equipment configuration. Noise power measurements were made in 25 kHz bandwidth channels at several representative center frequencies in three potential "Little LEO" downlink bands as shown in Table 2-1.

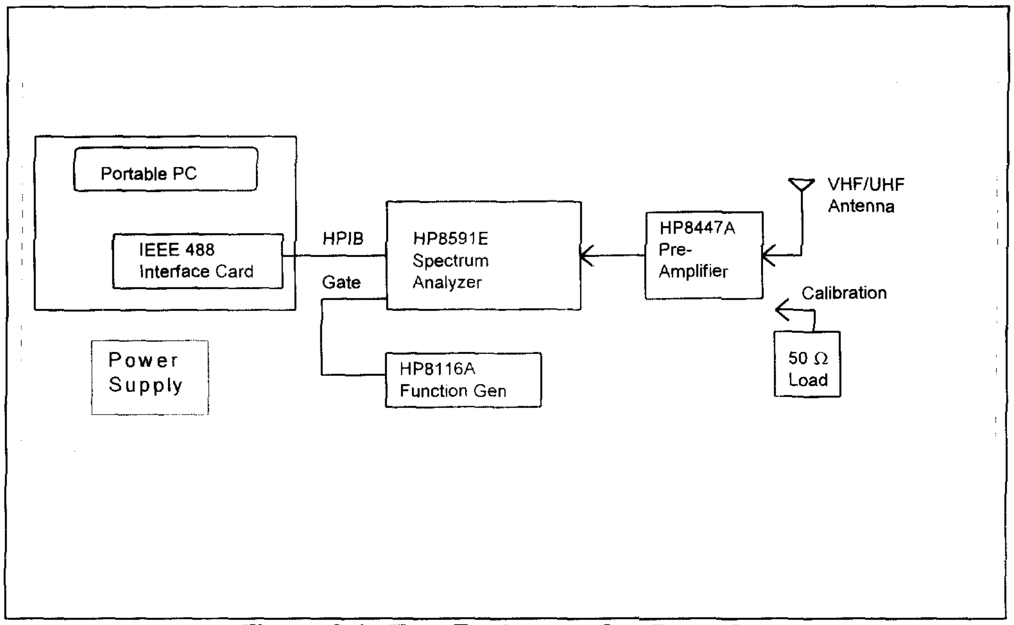

Figure 2-1. Test Equipment Configuration

Table 2-1. Measurement Center Frequencies and Corresponding Frequency Bands

Band	Center Frequencies
137 - 138 MHz	137.0125, 137.4175, 137.4445, 137.4725 MHz
387 - 390 MHz	388.1, 388.75 MHz
400.15 - 406 MHz	402.5, 405.237 MHz

An HP 8591E spectrum analyzer with a time gating option was used to perform the noise power measurements. The instrument settings were as follows:

Frequency	: noted in Table 2-1
Span	: 50 kHz
Sweep	: 167 msec
Resolution BW	: 3 kHz
Video BW	: 300 Hz
Trigger	: External

Gate Measurement : Turn ON at LEVEL TRIGGER
Power Meter : Power Measurement Utility in 25 kHz BW

A 1 Hz square wave with an amplitude of 1.5 V peak-to-peak and a DC offset of 0.74 V was generated by a function generator (HP8116A). This was used to provide a half-second burst window gating signal. The HP8447A preamplifier provides 7 dB noise figure, 20 dB gain, and has a 500 MHz bandwidth.

The measurement data collection was performed automatically using an IEEE 488 BUS, and the data was stored in a portable computer. The computer was used to monitor the spectrum analyzer's gated power measurements and collect 300 samples in each measurement set.

Prior to making each day's measurements, the noise floor of the preamplifier was calibrated. This was performed by installing a 50Ω load in place of the antenna at the input port of the HP8447A preamplifier. Three hundred samples were collected to measure the noise power of the preamplifier. All noise power measurements are presented in dB relative to the preamplifier's calibrated noise floor (kTB).

Table 2-2 provides a list of the test equipment used.

Table 2-2. Equipment List

	Model No.	Option	Description
1	HP8591E	105, 021	Spectrum Analyzer
2			Antenna VHF/UHF Band
3	PCMCIA-GPIB		IEEE 488 Interface Card
4	776670-01		LabView Software for IEEE 488 Card
5	HP8116A		Function Generator
6			486-33 Toshiba Notebook PC
7	HP8447A		Pre Amp, NF = 7 dB

Measurements were performed in both parked locations and while driving. In order to conduct these measurements, the setup was mounted on the truck shown in Figure 2-2. The antenna was mounted on the outside rear of the truck cab. The measurement equipment was located in a storage compartment mounted in the truck bed. The power supply was kept inside the cab of the truck. The locations and driving routes are provided in Tables 2-3 and 2-4, respectively.

Figure 2-2. Truck Used for Noise Measurements

Table 2-3. Locations where Measurements were Taken

Environment	Locations
Airport	Los Angeles International Airport parking structure
Industrial	El Segundo
Urban	Westwood parking lot
Rural	Chino Facility
Suburban	Van Nuys neighborhood
Harbor	Long Beach (berth 14)
Freeway	Downtown Los Angeles
Reference	Chino Hills, Chino, CA

Table 2-4. Driving Routes

Freeway	Freeway Name and Direction	Miles
Route 1	405S, 105E, 110N, 91E	40
Route 2	91W, 110S, 105W, 405N	40
Route 3	10E, 60E	50
Route 4	405S, Inglewood/El Segundo, 405N, Korea Town, Downtown, Pomona, Ontario, San Bernardino, Cherry Valley	160
Route 5	91E	50

In order to characterize the VHF/UHF antenna which was used in this study, its antenna factor was measured by an ANSI (American National Standards Institute) C63.4 certified laboratory located in Brea, CA. A reference antenna and the VHF/UHF antenna were located in an open field. Measurements were then taken for several relative positions of the antennas. The high and the low gain measurements are shown in Figure 2-3. As can be seen, there is a large variation in gain which is largely due to the multipath characteristics of the relative positions of the VHF/UHF antenna, truck, environment, and reference antenna.

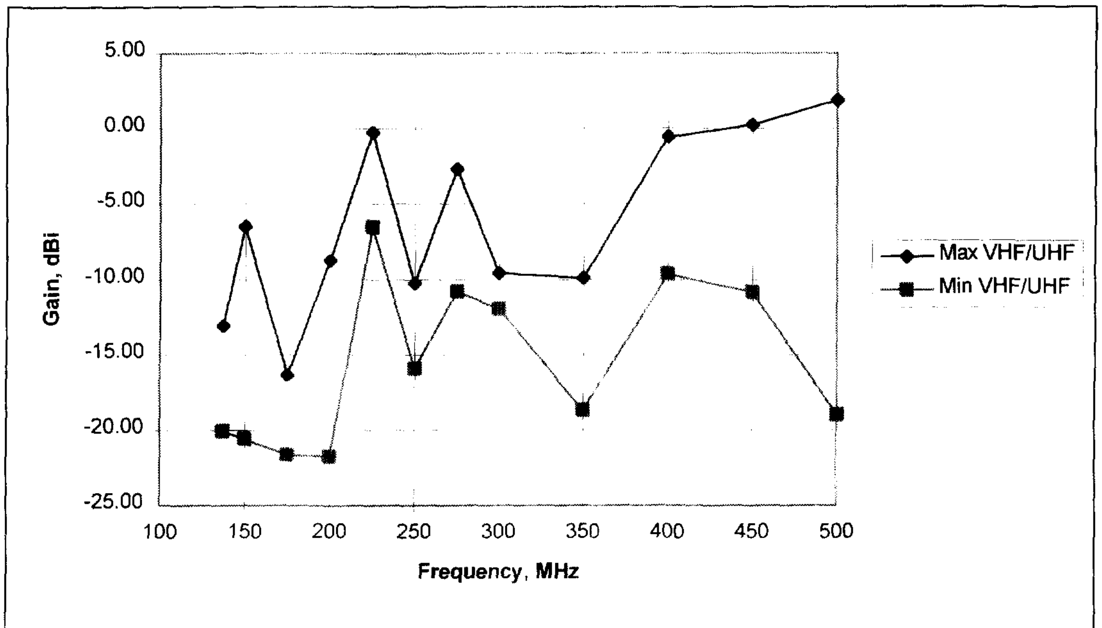

Figure 2-3 Antenna Gain

This shows that the VHF/UHF antenna can actually experience a large signal loss due to multipath characteristics. For example, at 137 MHz, the VHF/UHF antenna can experience as much as 15 dB additional signal loss in comparison with that of the wideband dipole antenna. While the noise measurements collected in this report reflect an average power measurement, the actual noise power level can vary by the difference between the VHF/UHF antenna gain and the wide-band dipole antenna gain as shown above.

2.1 Measurement Theory

The theory of the noise power measurements follows. Let B Hz denote the noise power measurement bandwidth at the band center frequency, f_c Hz. Let $\eta_0 = kT^o$ Watts/Hz denote the reference thermal noise power. For the measurement set-up, B = 25 kHz; thus, the thermal noise power is given by $\eta = kT^oB \cong -126$ dBm. Let N characterize the total noise power measured in the 25 kHz bandwidth. Clearly, this measured power, N, is random from measurement to measurement, and, mathematically speaking, is a random variable characterized by its cumulative distribution function $F_I(x)$, defined by

$$F_I(x) = P[N \leq x], \qquad 0 \leq x < \infty$$

where P[ ] denotes the probability of the event contained inside the brackets. Obviously, $0 \leq F_N(x) \leq 1$ for all x.

Define the total measured noise power to thermal noise power ratio as the normalized random variable

$$\frac{N}{\eta} = \frac{N}{kT^oB}$$

So that in decibels, this ratio assumes the form

$$Y = 10\log_{10}\left(\frac{N}{\eta}\right) = (N)_{dB} - \left(kT^oB\right)_{dB}$$

Now Y represents the measured noise power relative to the thermal noise power. In this report, this ratio will be referred to as the "power relative to kT^oB." Since the measured value of N is random from measurement to measurement, the random variable Y is also characterized by the cumulative distribution function for Y, given by:

$$F_Y(y) = P[Y \leq y], \qquad 0 \leq y < \infty$$

The values of $F_Y(y)$ at the measured noise power to thermal noise power ratio y represent the probability that Y is less than or equal to y. Clearly, $0 \leq F_Y(y) = P[Y \leq y] \leq 1$ for all y.

One main purpose of the measurement test set-up in Figure 2-1 is to collect noise power measurements as a function of time-of-day, environment, frequency band, etc., and to process these measurements so as to characterize the cumulative distribution function, $F_Y(y)$, and hence the noise power present in the Leo One USA communications channel. Perhaps of greater interest to the communications engineer is the characterization of the exceedence probability distribution; that is, the probability that the measurement Y is greater than a value, y. In probability terms, one requires characterization of the exceedence probability function

$$P[Y \geq y] = 1-F_Y(y)$$

This probability function varies from one to zero as y varies from 0 to infinity. In fact, the measurement test set-up is configured so as to collect the necessary statistical data which characterizes the exceedence probabilities. In this report, this probability will be referred to as the cumulative probability that the noise power will exceed y dB; it will be plotted versus thermal noise power N relative to $\eta = kT^{o}B$; i.e., $Y = (N/\eta)_{dB}$ for various environments, center frequencies, and time-of-day. Examples of the exceedence probability are presented in Appendix B.

From these plots, several probabilities will be of great interest. For example, if we set $P[Y \geq y] = 0.1$ and "solve" for the value of y (which we will call the 10% value $y_{0.1}$) which satisfies this probability equation, one can make the statement that 10% of the time the total noise power to thermal noise power ratio exceeds $y_{0.1}$. Similarly, letting $y_{0.9}$ denote the value of y which solves the equation $P[Y \geq y] = 0.9$, one can say that 90% of the time the measured value Y exceeds the determined 90% value, $y_{0.9}$. Furthermore, letting y_m denote the median value of the total noise power to thermal noise power ratio (i.e., the value of y that solves the equation $P[Y \geq y] = 0.5$), one can say that 50% of the time the total noise power to thermal noise power ratio Y exceeds y_m and 50% of the time the ratio is less than y_m.

Consider again 90% and 10% values, $y_{0.9}$ and $y_{0.1}$ respectively. Now the probability of the event $[y_{0.9} \leq Y \leq y_{0.1}]$ is found from

$$P[y_{0.9} \leq Y \leq y_{0.1}] = P[Y \leq y_{0.1}] - P[Y \leq y_{0.9}]$$

This can be written in terms of the measured cumulative probability distribution as

$$P[y_{0.9} \leq Y \leq y_{0.1}] = F_Y(y_{0.1}) - F_Y(y_{0.9}) = 0.8$$

One can interpret this measurement as meaning that 80% of the time the total noise power to thermal noise power ratio falls in the interval $[y_{0.9}, y_{0.1}]$. For most of the measurements taken, the difference $(y_{0.1} - y_{0.9})$ is small. Thus, one can conclude that the median value y_m can be used for system design purposes. In other words, with relatively high confidence, the total noise power to thermal noise power ratio is very close to y_m.

3.0 Measurement Locations

Figure 3-1 provides a map of the Los Angeles area showing the measurement locations. A brief description of each location follows. Photographs are shown in the indicated figures.

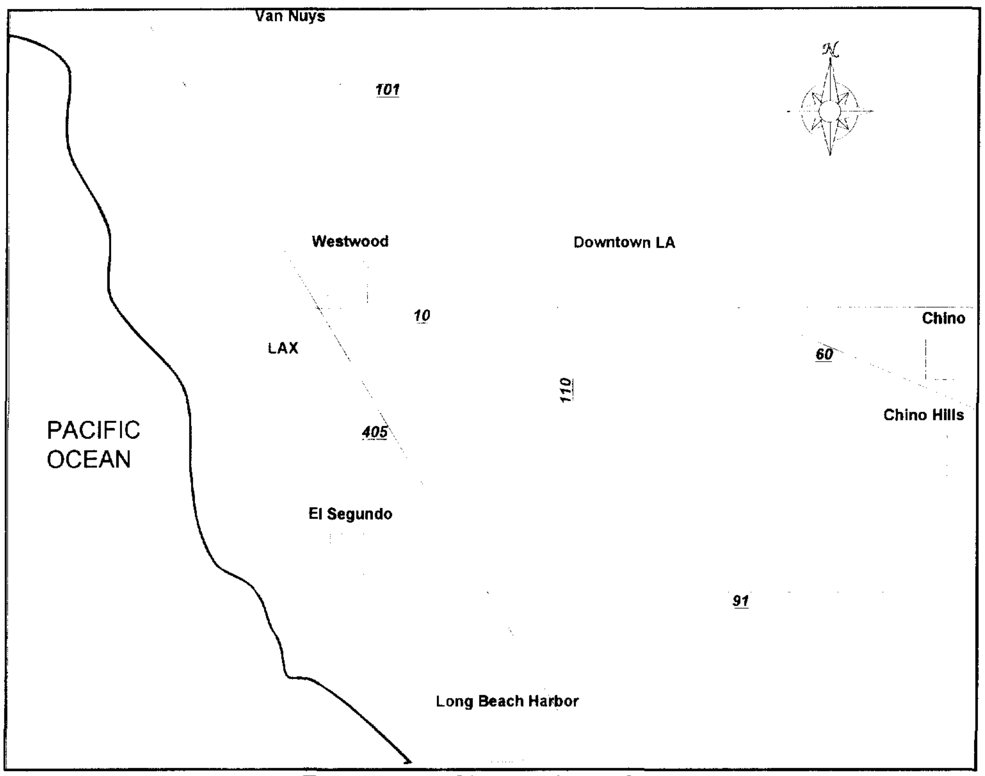

Figure 3-1. Chosen Locations

3.1 Airport - Los Angeles International Airport (Figure 3-2)

The top floor of LAX parking structure Number 1 was chosen for the airport environment. This location provided an open view of Terminal 1, the air traffic control tower, other parking lots, a restaurant, and a hotel, as well as arriving and departing flights. Measurements were collected on 9 May 1995 from 1044 to 1614 PDT.

3.2 Industrial - Aviation Blvd., El Segundo (Figure 3-3)

This location was chosen due to its proximity to the industrial Northrop factory and a busy boulevard. This location provided a street-level view of the factory, busy intersection, residential neighborhood, and several restaurants. Measurements were collected on 10 May 1995 from 1017 to 1547 PDT

3.3 Urban - Westwood (Figure 3-4)

A street-level parking lot was chosen for the Urban location. The parking lot was situated in the middle of a commercially active area. From this location, several high-rise buildings can be seen, as well as a three-floor parking structure. Measurements were collected on 11 May 1995 from 1006 to 1538 PDT.

3.4 Rural - Chino (Figure 3-5)

For the rural environment, a long quiet residential street was chosen. The houses on this street were "ranch style" with large open properties. This street was lined with trees and bushes. Farm animals, such as chickens, could be heard. Measurements were collected on 18 May 1995 from 1108 to 1933 PDT.

3.5 Suburban - Van Nuys (Figure 3-6)

This was a typical residential street with wood frame houses lining both sides. Cars were parked in driveways, and medium-sized trees were visible. Measurements were collected on 16 May 1995 from 1023 to 1849 PDT.

3.6 Harbor - Long Beach (Figure 3-7)

The harbor environment was a location near berth 14 in Long Beach. From this location, views of the water, berth 14, harbor equipment (e.g. large cranes), and a freeway (710) were visible. Measurements were collected on 12 May 1995 from 1045 to 1616 PDT.

3.7 Freeway - I-10 (Figure 3-8)

A parking lot, near Downtown LA, with a direct view of the busy Interstate 10 freeway was selected. This location provided an almost level view of the freeway. Measurements were collected on 15 May 1995 from 1021 to 1847 PDT.

3.8 Reference - Chino Hills (Figure 3-9)

For the reference site, a quiet location was chosen. Situated in the Chino area, the reference location was surrounded by brush covered hills. No power transmission lines were visible. Measurements were collected on 13 May 1995 from 1002 to 1531 PDT.

Figure 3-2. Los Angeles International Airport

Figure 3-3. Aviation Blvd, El Segundo, CA (Industrial)

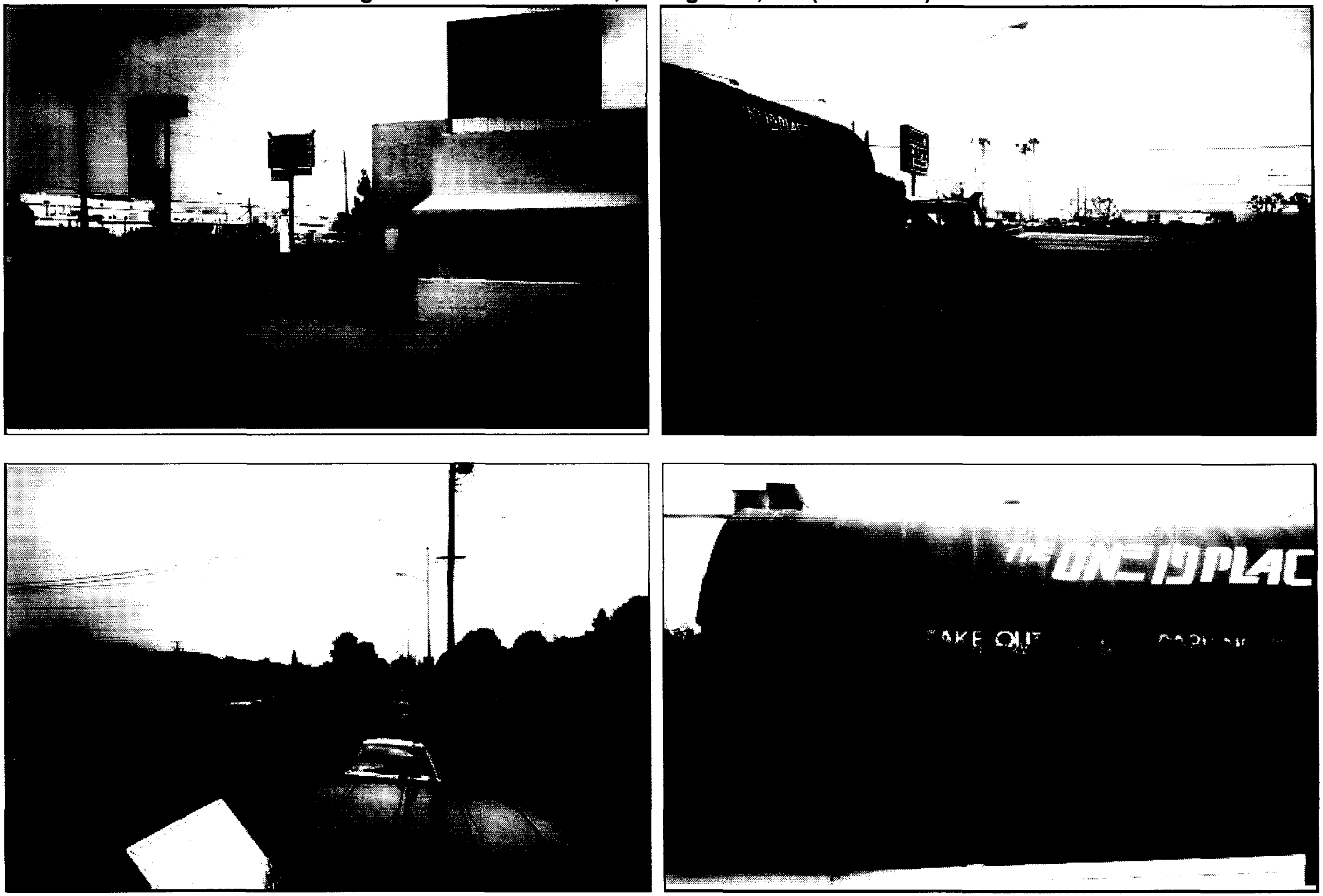

Figure 3-4. Westwood, CA (Urban)

Figure 3-5. Chino, CA (Rural)

Figure 3-6. Long Beach Harbor

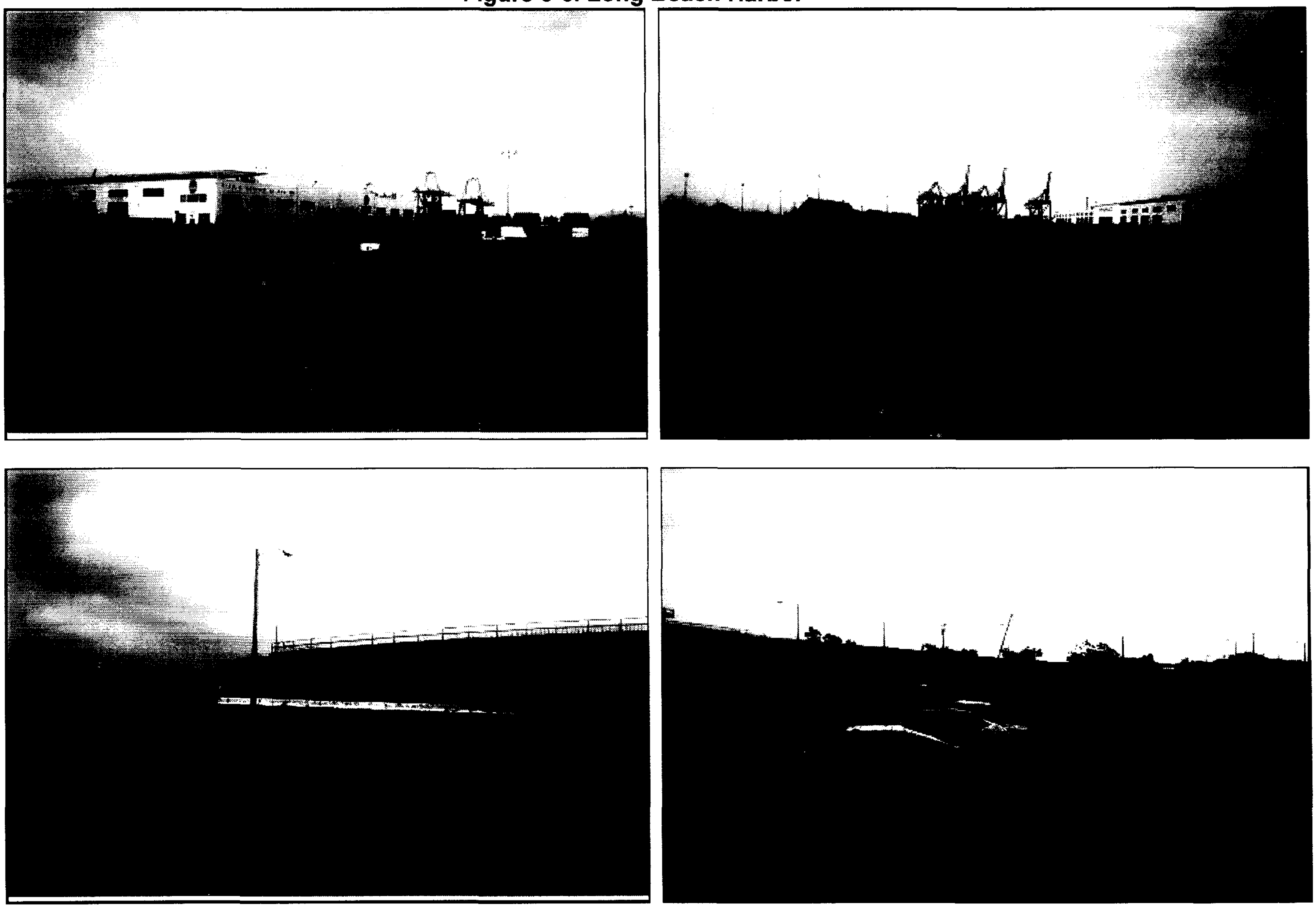

Figure 3-7. Van Nuys, CA (Suburban)